

Formation of trade networks by economies of scale and product differentiation

Chengyuan Han,^{1,2,*} Malte Schröder,^{3,†} Dirk Witthaut,^{1,2,‡} and Philipp Böttcher^{1,§}

¹*Forschungszentrum Jülich, Institute for Energy and
Climate Research (IEK-STE), 52428 Jülich, Germany*

²*Institute for Theoretical Physics, University of Cologne, Köln, 50937, Germany*

³*Center for Advancing Electronics Dresden (cfaed) and Institute for Theoretical Physics,
Technische Universität Dresden, Dresden, 01062, Germany*

(Dated: December 7, 2022)

Abstract

Understanding the structure and formation of networks is a central topic in complexity science. Economic networks are formed by decisions of individual agents and thus not properly described by established random graph models. In this article, we establish a model for the emergence of trade networks that is based on rational decisions of individual agents. The model incorporates key drivers for the emergence of trade, comparative advantage and economic scale effects, but also the heterogeneity of agents and the transportation or transaction costs. Numerical simulations show three macroscopically different regimes of the emerging trade networks. Depending on the specific transportation costs and the heterogeneity of individual preferences, we find centralized production with a star-like trade network, distributed production with all-to-all trading or local production and no trade. Using methods from statistical mechanics, we provide an analytic theory of the transitions between these regimes and estimates for critical parameters values.

I. INTRODUCTION

Trade networks are essential to today's international economy [1, 2]. From supply chains to financial transactions, goods and values are exchanged among almost every region on Earth. The importance of economic connectivity and complexity becomes most obvious in case of a disturbance: The world financial crisis of 2007/2008 emerged after inter-bank claims and liabilities had been growing for decades, enabling a rapid spread of financial risks [3, 4]. Similarly, disruptions of global transportation networks due to the Covid-19 pandemic have led to a substantial loss of production in various regions [5].

The emergence of connectivity and the structure of networks are essential topics in complexity science [6–8]. Traditionally, ensembles of random networks have been used to describe essential features of real-world networks such as the small-world effect of the emergence of hubs [9, 10]. On the one hand, percolation theory enables far-reaching insights into the formation and robustness of ensembles of networks [11]. On the other hand, optimization models have been used to describe the structure of biological networks [12, 13], assuming that evolution created structures that provide a certain function in an optimal way. Both

* ch.han@fz-juelich.de

† malte.schroeder@tu-dresden.de

‡ d.witthaut@fz-juelich.de

§ p.boettcher@fz-juelich.de

approaches are of limited use in the modeling of economic networks, where links are neither established at random, nor following a single, global objective. Instead, links are established deliberately on the basis of individual decisions.

The emergence of trade is a central subject of economics. In the celebrated Ricardian model, trade patterns are determined by the regional differences in productivity [14]. Advanced models have revealed essential factors fostering the emergence of trade in more detail [1, 15], in particular lower transportation costs and higher manufacturing shares. Furthermore, economic scale effects foster the centralization of production, as they lead to lower production costs for large producers and thus to advantages in competition.

However, transportation and production costs are not the only attributes that determine economic interactions and trade. Discrete choice theory investigates how economic agents reach a decision on the basis of both observed and unobserved attributes [16, 17]. The agents' preferences vary, in particular with respect to the unobserved attributes, and so do the agents' choices. Thus, discrete choice models are intrinsically stochastic, describing the probability of choice on an individual level or the demand for certain goods or brands on an aggregate level. As a consequence, populations of heterogeneous consumers demand differentiated goods [18, 19].

In this article we establish a model for the formation of trade networks combining essential concepts of economics and statistical physics. Trade links are established by the decisions of individual agents taking into account complex cost functions as well as differentiated preferences. The cost functions incorporate economic scale effects, making the decision problems nonlinear and interdependent. Statistical physics guides the numerical solution of the problem as well as the analysis of the results. We compute the 'phase diagram' of the emergent trade network using a self-consistent method and provide an approximate analytic theory for the transitions between different regimes of the emerging trade network. The current article generalizes previous models [20, 21] which neglected product differentiation and focused solely on percolation aspects.

II. MODELS AND METHODS

A. A model of emerging trade networks

We introduce a model for the emergence of trade networks due to individual decisions of multiple agents. Agents decide where to purchase goods to satisfy their demand based on two goals: (i) the reduction of costs and (ii) the preference for a diverse supply.

To formalize this model, we consider a set of nodes or vertices $i = 1, \dots, N$ representing a well-defined spatial unit. Each node i comprises a set of agents who want to satisfy their demand D_i for a certain class of goods by either local production or by purchases from other nodes. We denote the purchases that node i makes from a node j as S_{ji} , where S_{ii} gives the amount of local production such that

$$\sum_{j=1}^N S_{ji} = D_i. \quad (1)$$

The agents at node i decide how to satisfy the demand by optimizing the purchases S_{ji} , $j \in \{1, \dots, N\}$ to maximize their utility. The aggregated utility function $\mathcal{U}_i(S_{1i}, \dots, S_{Ni})$ of a node i includes two terms representing the two preferences introduced above: (i) the costs K_i that shall be minimized and (ii) a function H_i that measures the diversity of the supply that shall be maximized. We assume that the two terms are included as a weighted sum with a tunable weighting factor \mathcal{T} such that we obtain

$$\mathcal{U}_i(S_{1i}, \dots, S_{Ni}) = \mathcal{T} H_i(S_{1i}, \dots, S_{Ni}) - K_i(S_{1i}, \dots, S_{Ni}). \quad (2)$$

Here, we use Gibbs entropy for the function H_i to measure the diversity of the supply,

$$H_i = - \sum_{j=1}^N \frac{S_{ji}}{D_i} \ln \frac{S_{ji}}{D_i}, \quad (3)$$

where S_{ji}/D_i gives the probability of finding a purchase made by a single agent of node i at node j . Hence, we can view this quantity as equivalent to the probability of a micro-state in statistical physics.

The cost function K_i of a node i includes both transportation and production costs, where the latter is subject to scale effects [20, 21]. We can further disentangle the costs according to the node j , from which a good is purchased, such that the cost function reads

$$K_i = \sum_{j=1}^N K_{ji}^P + K_{ji}^T, \quad (4)$$

where the superscripts P and T refer to production and transportation, respectively.

The production costs K_{ji}^P scale with the purchases S_{ji} . Denoting the production costs per unit at a node j by p_j^P , we thus have

$$K_{ji}^P = p_j^P \times S_{ji}. \quad (5)$$

Production costs are typically affected by economies of scale: The higher the total production, the lower the production costs per unit. Here, we take this effect into account by a linearly decreasing function

$$p_j^P(S_j) = b_j - aS_j, \quad (6)$$

where

$$S_j = \sum_i^N S_{ji} \quad (7)$$

is the total production at a node j . The total production at the largest supplier in the system is denoted as

$$S^* = \max\{S_1, S_2, \dots, S_N\} \quad (8)$$

and characterizes the degree of centralization of production. We assume that the parameters b_j and a are such that $p_j^P(S_j) > 0$ is satisfied for all purchases. Transportation costs K_{ji}^T also scale with the purchases S_{ji} . They are not subject to scale effects, but depend on the distance E_{ji} of the two nodes j, i such that we obtain

$$K_{ji}^T = p^T E_{ji} S_{ji}. \quad (9)$$

The transportation network and the distance E_{ji} are discussed in detail below. The symbol p^T denotes the transportation costs per unit of goods and per unit of distance. This quantity typically decreases over time as the technology in the transportation sector advances.

In summary, we have introduced a model that describes different preferences of the agents as well as a complex cost function featuring production costs, transportation costs and economies of scale. The model includes three global parameters: (i) the parameter \mathcal{T} in the utility function that describes whether the agents at a certain node put more weight on a diverse supply (high \mathcal{T}) or on low costs (low \mathcal{T}), (ii) the specific transportation costs p^T and (iii) the strength of economic scale effects a .

If the specific transportation costs p^T are high and the preference for a diverse supply \mathcal{T} is low, we always find local production, that is $S_{ii} = D_i$ and $S_{ij} = 0$ for $i \neq j$. A trade

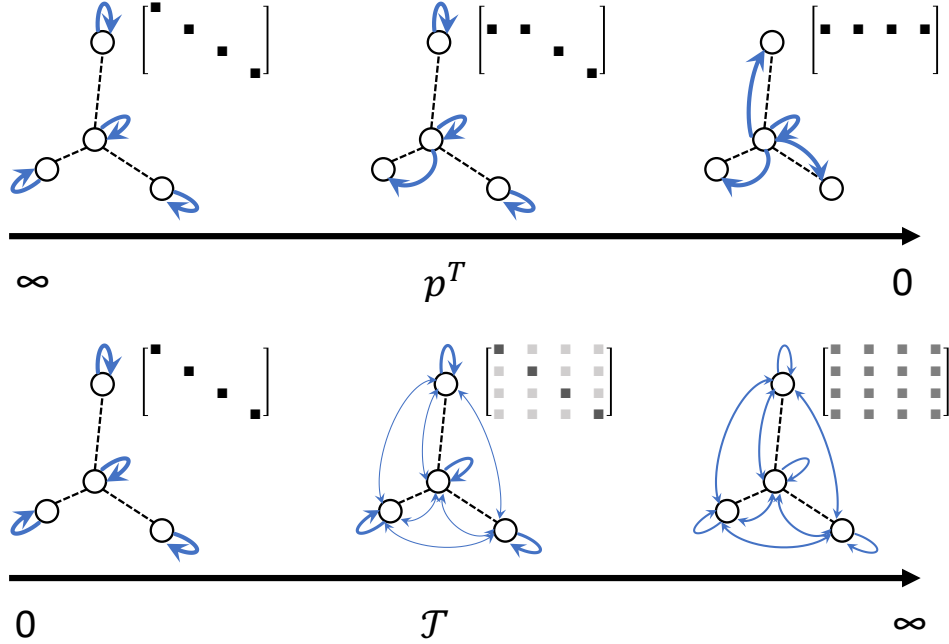


Figure 1. Routes to the emergence of a trade network. Upper row: If the specific transportation costs p^T decrease, it becomes cheaper for nodes to satisfy their demand by imports from cheaper neighbors than by local production. Emergence of a one-to-all trade network is predominantly driven by economic scale effects. Bottom row: If the preference for a diverse supply \mathcal{T} increases, agents are willing to pay additional transportation costs to import a diverse set of goods and an all-to-all trade network emerges. The figures illustrate the existing transportation network (black) as well as the emerging trade network (blue), while the insets depict the resulting matrix of purchases S_{ji} .

network can then emerge through two different mechanisms as sketched in figure 1: (i) If p^T decreases it becomes cheaper for a node to satisfy its demand by imports than by local production. This route to trade is strongly promoted by the scale effects of production [20]. Once a node starts to export goods, production costs per unit decrease, facilitating further exports. (ii) If \mathcal{T} increases, the preference for a diverse supply causes agents to more evenly distribute their purchases despite additional transportation costs. Eventually, an all-to-all connected network of trades emerges. We study the different routes to the emergence of a trade network in detail in sections III and IV.

We finally note that the negative utility function, $-\mathcal{U}_i = K_i - \mathcal{T}H_i$, has a similar form as the Helmholtz free energy in the study of closed thermodynamic systems. Because of this

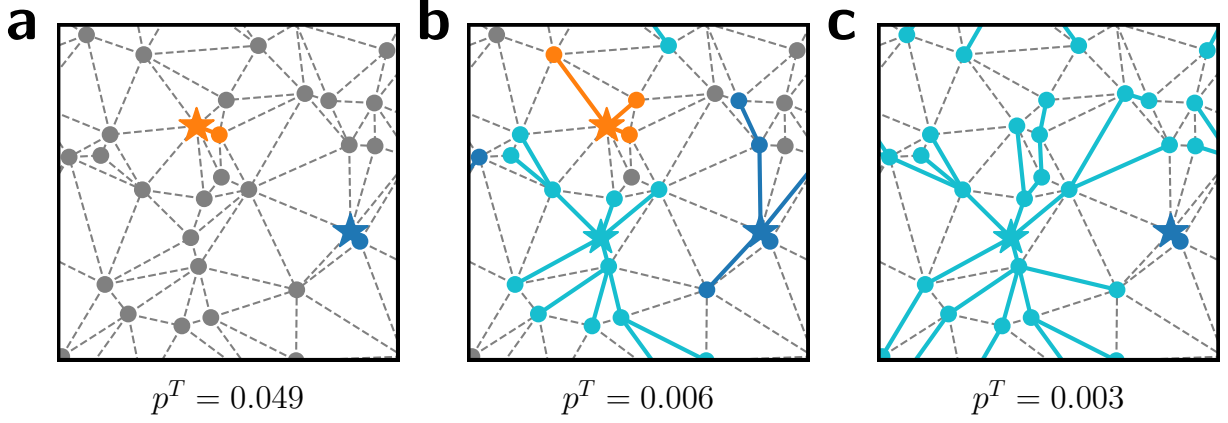


Figure 2. The transportation network and the emerging trade network during the centralization of production. Symbols and dashed lines show the nodes and the edges of the transportation network, while solid lines in different colors indicate clusters in the emerging trade network. Colored stars indicate nodes that export goods to all nodes in the respective cluster, shown in the same color. Grey nodes supply only themselves and gray dashed lines indicate transportation routes that are not being used. As the transportation cost decreases from panel **a** to **c**, the cluster size of the largest supplier grows until it encompasses almost the entire network. Parameters are $\mathcal{T} = 0$ and $a = 10^{-3}$.

structural similarity, we refer to the weighting factor \mathcal{T} as the effective temperature of the economic system in the following. The similarities to statistical physics will further guide our analysis of the system and provide methods to quantitatively understand the transitions between different trade regimes.

B. Transportation and trade networks

The model introduced above describes the emergence of trades described by the purchases S_{ji} on a underlying transportation network, determining the transportation costs via the distances E_{ji} . To study the model numerically, we generate ensembles of geographically embedded transportation networks as follows. First, a number of nodes is placed uniformly at random in the unit square with periodic boundary conditions, which is equivalent to a two-dimensional torus. Second, these nodes are connected using Delaunay triangulation on the torus. The length of an edge (i, j) is given by the Euclidean distance of the terminal

nodes i and j with respect to the periodic boundary conditions. The distance E_{ji} from node j to node i is then given by the geodesic distance on the transportation network. Finally, the nodes are characterized by their demand, which is taken to be uniform for all simulations, $D_i = D = 1/N$, and by the parameter b_i , which is chosen uniformly at random from the interval $[1.005, 1.01]$ for each node.

Figure 2 shows an example of the generated transportation network as well as the emerging trade network from an exemplary simulation for $\mathcal{T} = 0$, $a = 10^{-3}$ and decreasing transportation cost p^T . For very high values of p^T the supply matrix is diagonal, $S_{ii} = D_i$ and $S_{ji} = 0$ for $j \neq i$, such that the trade network is fully disconnected. When p^T is gradually lowered, some nodes start to purchase their goods at other nodes, represented by colored stars. The emerging trade network is thus composed of clusters with a single supplier (identified by different colors in figure 2). For very small p^T , the production becomes increasingly centralized such that one cluster grows until it contains all nodes.

C. Equilibrium states and self-consistency conditions

Our model for the emergence of trade networks relies on a complex optimization approach. The agents at each node i will take their decisions individually to optimize the utility function \mathcal{U}_i . However, the N optimization problems are not independent because of the existence of scale effects. If a node i decides to purchase at another node j , this will reduce the production costs per unit p_j^P , which may in turn affect the decision of all other nodes. Hence, we have to determine the set of all purchases S_{ji} such that it represents a Nash equilibrium: No node i can further increase its utility function by changing its purchases S_{1i}, \dots, S_{Ni} while the purchases of all other nodes remain constant.

A method to solve this complex optimization model for the limiting case $\mathcal{T} = 0$, when a node i purchases only from a single supplier, was introduced by Schröder et al. [20]. An important finding is that multiple equilibria can coexist, which gives rise to hysteresis effects. Here, we show how to extend this approach to the case $\mathcal{T} > 0$, when nodes distribute their purchases, using a self-consistency approach.

In a Nash equilibrium, every node i maximizes its utility function $\mathcal{U}_i(S_{1i}, \dots, S_{Ni})$ under the constraint $\sum_j S_{ji} = D_i$ assuming that the purchases of all other nodes are fixed. We determine this maximum using the method of Lagrangian multipliers, leading to the

conditions

$$\frac{\partial}{\partial S_{ji}} \left[\mathcal{U}_i - \lambda \left(\sum_{\ell=1}^N S_{\ell i} - D_i \right) \right] = 0 \quad (10)$$

for all $i = 1, \dots, N$. Solving these conditions yields

$$\frac{S_{ki}}{D_i} = \frac{\exp(-D_i \tilde{p}_{ki}^{\text{eff}}(S_{ki})/\mathcal{T})}{\sum_{k=1}^N \exp(-D_i \tilde{p}_{ki}^{\text{eff}}(S_{ki})/\mathcal{T})}. \quad (11)$$

with the short-hand

$$\tilde{p}_{ji}^{\text{eff}} = b_j + p^T E_{ji} - a \left(S_{ji} + \sum_{\ell=1}^N S_{j\ell} \right). \quad (12)$$

In the case of large networks and with sufficiently diverse purchases, the term S_{ji} is typically negligible in comparison to the sum over N terms $S_{j\ell}$. Hence, we are lead to the approximation $\tilde{p}_{ji}^{\text{eff}} = p_{ji}^{\text{eff}}$ with

$$p_{ji}^{\text{eff}} := (b_j - a S_j) + p^T E_{ji} = \frac{K_{ji}^P + K_{ji}^T}{S_{ji}}. \quad (13)$$

This expression equals the cost per unit and can be interpreted as the *effective price* which agents at node i would have to pay to purchase from node j .

Equations (11) and (13) have to be satisfied for all nodes $i \in \{1, \dots, N\}$ simultaneously. We thus find that the entire system is in an equilibrium state if all purchases follow a Boltzmann distribution given the corresponding equilibrium effective prices p_{ji}^{eff} .

D. Microscopic interpretation

Before we proceed to the numerical analysis of equilibrium states, we provide another more microscopic interpretation of the Boltzmann distribution (11). Discrete choice theory considers the individual agents or consumers which may choose from different discrete options. The preferences of the individuals vary leading to product differentiation [16–18].

A single agent a at node i can choose to purchase a good from different nodes $k \in \{1, \dots, N\}$ at different effective prices p_{ki}^{eff} . However, the price is not the only factor that determines consumer behavior and preferences generally differ. Hence, the utility of an individual agent a is written as

$$\mathcal{U}_a(k) = p_{ki}^{\text{eff}} + \zeta \epsilon_k, \quad (14)$$

the individual differences ϵ_k are typically unknown a priori and are thus modeled as random variables. The parameter $\zeta > 0$ measures how strongly preferences vary between individual

agents. A common assumption in the economic literature is that the ϵ_k are independent and identically Gumbel distributed, which leads to the classic multinomial logit model [18]. The probability of an agent r at node i choosing alternative k is then given by

$$\mathcal{P}_r(k) = \frac{\exp(-p_{ki}^{\text{eff}}/\zeta)}{\sum_{k=1}^N \exp(-p_{ki}^{\text{eff}}/\zeta)}. \quad (15)$$

The expected value of the cumulative purchases of node i from node k are thus given by

$$S_{ki} = D_i \frac{\exp(-p_{ki}^{\text{eff}}/\zeta)}{\sum_{k=1}^N \exp(-p_{ki}^{\text{eff}}/\zeta)}, \quad (16)$$

which coincides with equation (11) if we identify $\zeta = \mathcal{T}/D_i$.

E. Numerical solution

In a Nash equilibrium, purchases and effective prices are linked via the self-consistency conditions (13) and (11). We now establish a numerical scheme to compute this equilibrium state as a function of the system parameter. Starting from a suitable initial guess for the purchases S_{ji} , we compute the resulting effective prices (13). Given these prices we can directly compute a new value for the purchases (11). This procedure is iterated until no further changes in the purchases occur. Once the iteration converged, the resulting state satisfies both conditions (13) and (11) simultaneously such that we arrived at an equilibrium.

We emphasize once again that the model can support multiple equilibrium states. In such a situation it depends on the initial guess which one is found and if the iteration terminates at all. In the numerical simulations, we use the following algorithm to compute how the equilibrium states depends on the parameters a , p^T and \mathcal{T} :

1. We fix a value of $a > 0$ and a transportation network as described above. We set $D_i = 1/N$ for all nodes such that, when the production is fully centralized at a single node, the total production at this node is 1. In the simulations, we use $N = 300$ unless stated otherwise.
2. We start at $\mathcal{T} = 0$ and $p^T = \infty$, where the equilibrium state is given by $S_{ii} = D_i$ and $S_{ji} = 0$ for $j \neq i$, i.e. fully local production.
3. We then compute the equilibrium states along the line $\mathcal{T} = 0$ by decreasing p^T to zero. This computation follows the semi-analytic algorithm introduced in [20].

4. We define a grid of values for p^T and \mathcal{T} for which the supply matrix S_{ji} is to be computed. We choose the minimum (maximum) value of p^T such that production is fully centralized (local) for $\mathcal{T} = 0$. The step size is chosen uniform on a logarithmic scale. We then compute the equilibrium states as a function \mathcal{T} and p^T :
 - (a) For each value of p^T on the grid, we proceed from $\mathcal{T} = 0$ to $\mathcal{T} = \mathcal{T}_{\max}$.
 - (b) For a given value of p^T and \mathcal{T} we start from an initial guess for the purchases S_{ji} . For $\mathcal{T} > 0$ we use the solution for the previous, smaller value of \mathcal{T} . For $\mathcal{T} = 0$ the exact solution S_{ji} is known from the step 3.
 - (c) We compute the effective prices p_{ji}^{eff} from equation (13) and update the purchases S_{ji} using equation (11).
 - (d) We iterate this procedure until it converges. Convergence is assumed when the Frobenius norm of the difference of the previous and the updated purchase matrix decreases below 10^{-8} .
5. The procedure is repeated for different random realizations of networks to average out the impact a single network might have on the position and behavior at the phase transition.

III. PHASE DIAGRAM OF THE TRADE NETWORK

How do the decisions of individual agents lead to the emergence of trade? In this section we provide an overview of the emerging trade networks and how they depend on the preferences of the agents, the properties of the transportation network, and the economic scale effects. To this end, we compute the equilibrium purchases S_{ki} using the self-consistent method introduced in section II E as a function of the parameters p^T , \mathcal{T} , and a . We average over 100 random realizations of the transportation network model (cf. section II B) to map out the typical behavior independent of the randomly chosen network. Single realizations will be treated in a subsequent section. For the sake of simplicity we set $D_i = D = 1/N$ in all simulations as discussed above.

Figure 3 shows two macroscopic observables that characterize the emerging trade network

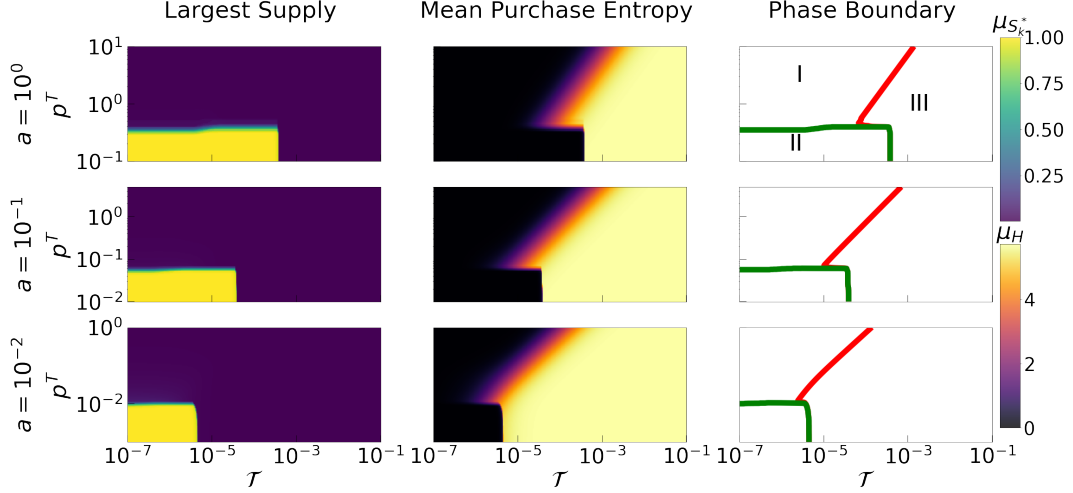


Figure 3. Phase diagrams of the emerging trade networks for different values of the scale effects a . The left column shows the production of the largest supplier in the system μ_S , and the middle column shows the mean purchase entropy μ_H . Results for μ_S and μ_H are averaged over 100 random realizations of the transportation network. Based on these observations, we identify three phases of the emerging trade network shown in the right column: (I) A phase of local production when the specific transportation costs p^T are high and the effective temperature \mathcal{T} is low. (II) A phase with centralized production, i.e. large $\lim_{\mathcal{T} \rightarrow 0} \lim_{p^T \rightarrow 0} \mu_S = 1$, for small values of both p^T and \mathcal{T} . (III) A phase with diversified production, i.e. high entropy $\lim_{\mathcal{T} \rightarrow \infty} \mu_H = \ln(N)$, for large values of \mathcal{T} . A definition and analysis of the phase transition is provided in the main text.

on large scales. The normalized maximum production,

$$\mu_S = \langle S^* \rangle, \quad (17)$$

quantifies the degree of centralization of the production, where the brackets denote the average over the transportation network ensemble. If μ_S is close to unity, the production is strongly centralized at a single node. The average entropy

$$\mu_H = \left\langle N^{-1} \sum_{i=1}^N H_i \right\rangle \quad (18)$$

measures the diversity of supply as described in section II A.

Based on the observables μ_S and μ_H , we identify three different regions in parameter space leading to qualitatively different patterns of the emerging trade networks:

- I. If the specific transportation costs p^T are high and the effective temperature \mathcal{T} is low,

we have

$$\lim_{\mathcal{T} \rightarrow 0} \lim_{p^T \rightarrow \infty} \mu_S = \frac{1}{N} \quad \text{and} \quad \lim_{\mathcal{T} \rightarrow 0} \lim_{p^T \rightarrow \infty} \mu_H = 0. \quad (19)$$

That is, every node produces for its own demand and has only a single supplier. No trading takes place in this phase such that the purchase matrix is given by

$$\lim_{\mathcal{T} \rightarrow 0} \lim_{p^T \rightarrow \infty} S = \frac{1}{N} \begin{pmatrix} 1 & 0 & \dots & 0 \\ 0 & 1 & \dots & 0 \\ \vdots & \vdots & \ddots & \vdots \\ 0 & 0 & \dots & 1 \end{pmatrix}. \quad (20)$$

We refer to this phase as the *local production phase* in the following.

- II. If the unit transportation costs p^T decrease, while the effective temperature \mathcal{T} is still low, we find

$$\lim_{\mathcal{T} \rightarrow 0} \lim_{p^T \rightarrow 0} \mu_S = 1. \quad (21)$$

That is, the production becomes completely centralized at a single node j and the purchase matrix can be written as

$$\lim_{\mathcal{T} \rightarrow 0} \lim_{p^T \rightarrow 0} S = \frac{1}{N} \begin{pmatrix} 0 & \dots & 0 & \dots & 0 \\ 1 & \dots & 1 & \dots & 1 \\ \vdots & \vdots & \vdots & \vdots & \vdots \\ 0 & \dots & 0 & \dots & 0 \end{pmatrix}. \quad (22)$$

We refer to this phase as the *centralized production phase* in the following.

- III. If the effective temperature \mathcal{T} is high, the preference for a diverse supply is essential for the decisions of the agents. Hence, we observe a phase with an average entropy close to the maximum possible value,

$$\lim_{\mathcal{T} \rightarrow \infty} \mu_H = \ln(N). \quad (23)$$

In this phase every node purchases a similar amount of goods from every other node such that the purchase matrix reads

$$\lim_{\mathcal{T} \rightarrow \infty} S = \frac{1}{N^2} \begin{pmatrix} 1 & \dots & 1 & \dots & 1 \\ 1 & \dots & 1 & \dots & 1 \\ \vdots & \vdots & \vdots & \vdots & \vdots \\ 1 & \dots & 1 & \dots & 1 \end{pmatrix}. \quad (24)$$

We thus find a globally connected trade network, where every node produces the same amount of goods, $\lim_{\mathcal{T} \rightarrow \infty} \mu_S = 1/N$, as in phase I but exports and imports from all other nodes. We refer to this phase as the *diverse production phase* in the following.

For a better overview, we extract a comprehensive phase diagram from the values of μ_S and μ_H in our simulations as follows. For both quantities, we determine the minimum and maximum values found in the simulations and choose the midpoints of the respective intervals as a threshold value. We then compute the areas in the phase diagram, where the observables μ_S and μ_H are above or below the respective thresholds. The red and green lines in figure 3 depict the boundary between these areas. Together, they reveal the boundary between the different phases I, II and III.

The resulting phase diagram in figure 3 on the right shows most clearly how the equilibrium trade network depends on the parameters p^T and \mathcal{T} as well as the strength of the scale effects a . We find that the three phases exist for all values a , but the location and nature of the phase boundaries depend strongly on a . Scale effects foster a centralization of production, such that the parameter region corresponding to centralized production (phase II) increases with a .

We observe qualitatively different transitions between the three phases:

- The transition between local and diverse production (I-III) is smooth. The phase boundary is a straight line $p^T/\mathcal{T} = \text{const.}$
- The transition from local to centralized production (I-II) is rather sharp and the phase boundary is almost given by a horizontal line, i.e. a constant value of p^T . However, a slight incline of the phase boundary becomes visible for large a , such that the transition can in principle also be triggered by a decrease in \mathcal{T} .

In economic terms, centralization of production is driven by a reduction in the specific transportation costs p^T . This process is facilitated by scale effects, which make the transition occur earlier (i.e. for larger values of p^T) and more rapid. This scenario is mostly, but not perfectly, independent of the consumer preferences expressed by the parameter \mathcal{T} .

- The transition between centralized and diverse production (II-III) is also very sharp and the phase boundary is almost given by a vertical line, i.e. a constant value of \mathcal{T} .

In economic terms, a change in the nodes' preferences can trigger a transition at low specific transportation costs p^T . If the agents emphasize costs (low \mathcal{T}), production is centralized at a single node. If they emphasize diversity instead (high \mathcal{T}), the production is decentralized. Remarkably, the transition occurs abruptly as \mathcal{T} increases.

- A particular behavior is observed around the triple point of the phases I, II, and III. For certain values of \mathcal{T} , we find a non-monotonic behavior of μ_H . Decreasing the unit transportation costs first induces a transition from local to diverse production, and then a transition to centralized production. Hence, μ_H first increases and then decreases back to values around zero. We note, however, that the system can have multiple equilibria [20], of which only one is analyzed here.

IV. TRANSITIONS BETWEEN DIFFERENT REGIMES

We now investigate the transitions between the three phases of the trade network in more detail. We discuss the type of the transition and derive approximate analytic expressions for the locations of the phase boundaries.

A. From local to centralized production

The transition from phase I to phase II describes the centralization of production due to the costs of production versus transport, while the preference for a diverse demand does not play a central role. The remarkable feature of this transition is that it can be either continuous or discontinuous depending on the value of a [20]. A discontinuity is the direct consequence of scale effects in the production. If a node i chooses to purchase its goods at a node j instead of producing locally, the production costs per unit at node j decrease due to scale effects. If this decrease is strong enough, another node i' may also choose to buy at j , further decreasing the production costs per unit at this node. Eventually, we may find a cascade of decisions, where a large fraction of nodes simultaneously change their purchases and the production is centralized at node j .

We analyse the transition in more detail, starting from the simplest case $\mathcal{T} = 0$ [20]. If $a = 0$ (and $\mathcal{T} = 0$) the maximum production changes in discrete steps of D as p^T is reduced. To see this, consider a node i which chooses its purchases to minimize its total costs. For

$\mathcal{T} = 0$, node i always chooses a single supplier node. If node i chooses to buy at node j instead of a node ℓ , the effective price node i pays per unit changes by

$$\Delta p^{\text{eff}} = (b_j - b_\ell) + p^T(E_{ij} - E_{i\ell}). \quad (25)$$

Hence, a node i will change its purchases if $p^T = (b_j - b_\ell)/(E_{ij} - E_{i\ell})$. These values of p^T are distinct for all nodes and potential suppliers with probability 1, such that changes in the purchases occur only in single events at different values of p^T . Hence, in the thermodynamic limit $N \rightarrow \infty$ with constant total demand ND constant, the transition from phase I to phase II is continuous [20].

If a is large (and $\mathcal{T} = 0$), the transition is generally discontinuous in the following sense. If p^T is reduced, the maximum production S^* changes by a macroscopically large amount ΔS^* at a critical value of p^T . This is due to a cascade of decisions of the individual nodes: If a node i chooses to purchase from another node j instead of buying locally, the production costs per unit at node j decrease by an amount aD . This decrease may be sufficiently strong, to cause another node i' to also purchase from j instead of buying locally. In the end, a macroscopic fraction of the nodes decides to change its purchases simultaneously. We note that the difference between continuous or discontinuous transitions is not visible in figure 3, as the phase diagram shows the average over many random realizations of the underlying transportation network. In contrast, a clear difference is observed for a single realization as shown in Figure 4.

For extremely large values of a we may even find a complete centralization in a single event, i.e., $\Delta S^* = (N - 1)D$. We make this statement more precise now. To this end, we order the nodes $n \in \{1, \dots, N\}$ as follows. The nodes $(j, i) = (1, 2)$ are chosen such that they have the lowest value of $(b_j - b_i) + E_{ji}$, that is

$$(b_j - b_i) + E_{ji} \leq (b_m - b_n) + E_{mn}, \quad \forall m \neq n. \quad (26)$$

The remaining nodes $n \in \{3, \dots, N\}$ are ordered such that the series

$$(b_1 - b_n) + E_{1n} \quad (27)$$

is monotonically increasing. Furthermore, we assume that

$$(i - 1)E_{12} > E_{1i}, \quad \forall i \in \{3, \dots, N\}. \quad (28)$$

This condition is typically satisfied if the differences in the parameters b_i are small. Then we find the following statement: If scale effects are extremely strong,

$$a > \max_{i \in \{3, \dots, N\}} \frac{|(b_1 - b_i)E_{12} - (b_1 - b_2)E_{1i}|}{D[(i-1)E_{12} - E_{1i}]}, \quad (29)$$

the maximum production changes from $S^* = D$ to $S^* = ND$ when the transportation costs per unit are decreased below a critical value

$$p_{\text{crit}}^T = \frac{aD}{E_{12}}. \quad (30)$$

A proof of this statement is given in appendix A. For large a we may thus compute the critical point directly from the network topology and the local values b_i .

B. Impact of temperature on the centralization

A reduction in the specific transportation costs p^T generally leads to a centralization of production. But how does the preference for a diverse demand, measured by the parameter \mathcal{T} , affect this scenario? Simulation results for different values of \mathcal{T} and a are shown in Figure 4.

In the case of strong scale effects, $a = 10^0$, we observe almost no differences between the curves for different \mathcal{T} . In this case, the cost effects dominate the decision of the agents: The centralization of production leads to strong changes which outweigh any possible gain by a more diverse supply. In other words, the utility function (2) is dominated by the second term.

In contrast, a substantial impact is found in the case of weak scale effects, e.g. $a = 10^{-2}$. Not surprisingly, the preference of a diverse supply counteracts centralization. That is, more producers persist for higher values of the effective temperature \mathcal{T} such that the maximum production S^* is smaller. But surprisingly, the final step of the centralization process – the centralization at a single node – takes place in an even more abrupt way. Correspondingly, the entropy H first grows smoothly, showing that a diverse supply is established, until it drops sharply. We thus find that the preference for diversity delays the growth of the trade network, until the growth occurs in an ‘explosive’ way. Similar explosive effects were found for a variety of different models in percolation theory [22, 23].

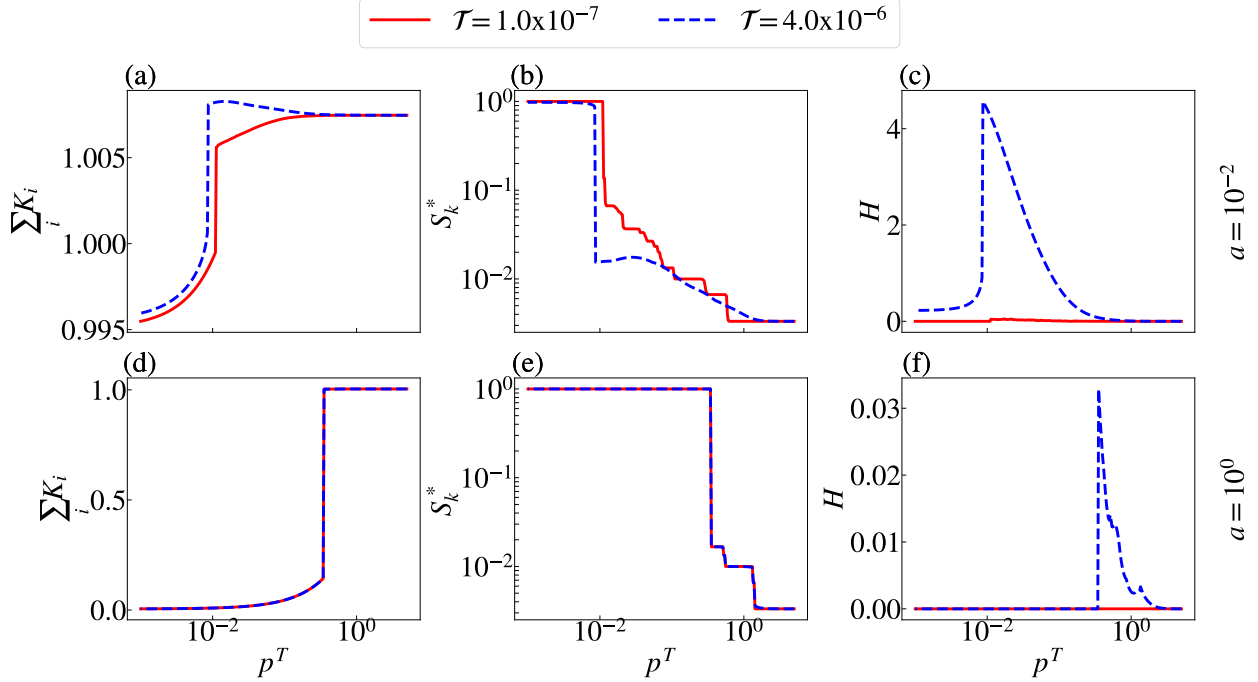


Figure 4. Transition from local to centralized production. Results are shown for a single instance of the transportation network, comparing the case of (a-c) weak scale effects and (d-e) strong scale effects as well as low and high effective temperatures (red solid vs. blue dashed line). We show (a,d) the total costs $\sum_i K_i$, (b,e) the production of the busiest node $S^* = \max_k S_k$ and (c,f) the entropy averaged over all nodes, $H = N^{-1} \sum_i H_i$.

C. From local to diverse production

The preference for a diverse supply induces a transition from local production to a diverse supply if either the effective temperature \mathcal{T} is increased or the specific transportation costs p^T are decreased. The boundary between the two regimes appears as a straight line with slope one in the double-logarithmic phase diagram (figure 3), except for the parameter region with both p^T and \mathcal{T} small leading to centralized production (phase II). In the following paragraphs, we provide a detailed analysis of the transition from local to diverse production and derive an analytical estimate for the location of the transition.

We first note that in both phases the local production of each node equals $S_j = D$. Hence, we assume that scale effects play no role for the transition and equation (11) for the purchases simplifies to

$$S_{ki} = D \frac{\exp[-D(b_k + p^T E_{ki})/\mathcal{T}]}{\sum_{k=1}^N \exp[-D(b_k + p^T E_{ki})/\mathcal{T}]}, \quad (31)$$

assuming $D_i = D$ as above. The differences in the local parameters b_k are small compared to $p^T E_{ki}$ in all simulations and can thus be neglected in the following analysis. We conclude that the transportation costs parameter p^T and the effective temperature \mathcal{T} enter only via the ratio

$$\beta = D p^T / \mathcal{T}. \quad (32)$$

Hence, also the entropy H will depend on p^T and \mathcal{T} only via the ratio β and the phase boundary is given by a straight line

$$p^T / \mathcal{T} = D^{-1} \beta_{\text{crit}} = \text{const.} \quad (33)$$

Indeed, the numerical simulations presented in figure 3 confirm this finding. The boundary between phases I and III is a straight line as long as p^T and \mathcal{T} are large enough such that no centralization occurs, i.e., far away from phase II.

The second conclusion we draw from the expression (31) is that we can treat all nodes $i = 1, \dots, N$ separately. We note that this assumption is strictly true only for $a = 0$, while it represents a useful approximation for $a > 0$. Indeed, the success of this assumption is surprising from a conceptual view at first glance. If a node i would independently redistribute its purchases, this would invalidate the assumption $S_j \approx D = \text{const.}$ which allowed us to neglect scale effects and treat all nodes separately. This apparent contradiction is resolved as follows: Typically, The decision of a node i to purchase from j is mirrored by a simultaneous decision of j to purchase at i if b_i and b_j do not differ too much. Hence, the decisions are not independent a priori but their effect cancels out such that the decisions of the nodes effectively separate and can be treated independently in the calculation.

Using these assumptions, we now provide an explicit approximate expression for the entropy H_i and the critical parameter β_{crit} . We first note that the entropy can be rewritten as (cf. appendix B)

$$H_i = -\frac{\partial}{\partial \beta^{-1}} \left[-\beta^{-1} \ln(Q_i) \right], \quad (34)$$

where

$$Q_i = \sum_{j=1}^N e^{-\beta E_{ji}} \quad (35)$$

can be interpreted as a partition function and the expression in the bracket as a free energy. To evaluate the Q_i , we just need the information of how many nodes are found at a given

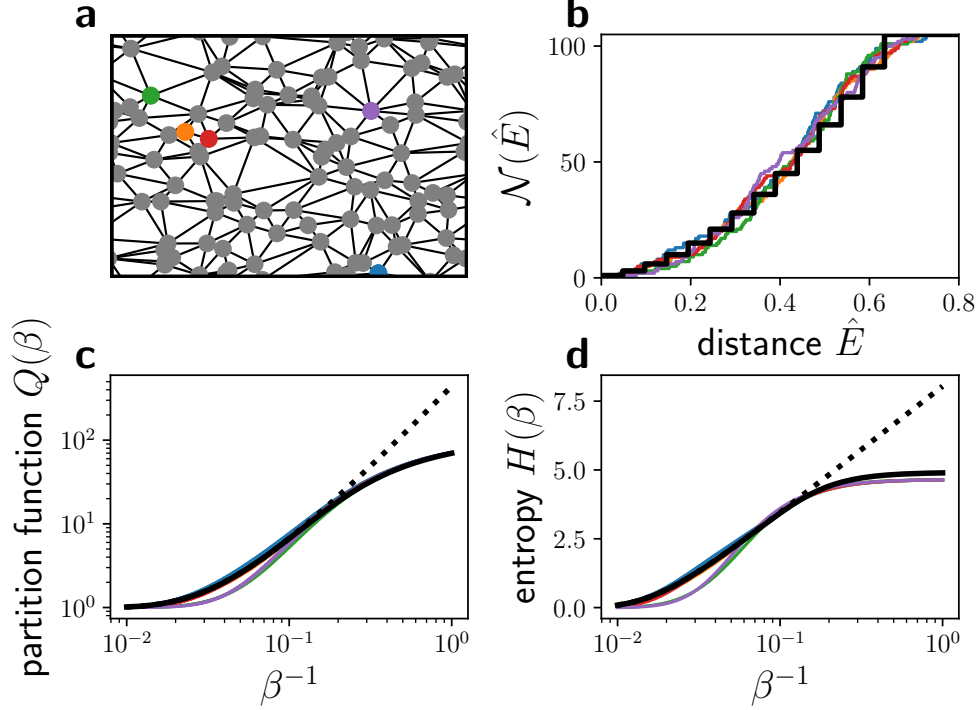


Figure 5. Transition between local and distributed production in a sample network. (a) Network structure of the sample network with $N = 105$ nodes. Five nodes were selected at random for further analysis (color coded). (b) The counting function $\mathcal{N}(\hat{E})$ counts the number of nodes with a distance $\leq \hat{E}$. We show $\mathcal{N}_i(\hat{E})$ for the five selected nodes (thin colored lines) in comparison to the analytic approximation (37) (thick black line). (c,d) The partition function (35) and the entropy (34) for the five selected nodes (thin colored lines) compared to the analytic approximation (38) (thick black line). On average, we find a very good agreement. For low temperatures, the partition function and entropy can be approximated by the expressions (39) and (40) (dotted black line).

distance E . We encode this in the counting function

$$\mathcal{N}_i(\hat{E}) = \sum_{j=1}^N \Theta(\hat{E} - E_{ij}), \quad (36)$$

where Θ denotes the Heaviside function. Notably, the function (36) can be interpreted as an integrated density of states.

To obtain an analytic approximation for Q_i , we have to approximate \mathcal{N}_i by a function that keeps the essential properties but allows to carry out the sum in equation (35) in closed form. Three properties have to be taken into account: (i) The function \mathcal{N}_i scales quadratically with \hat{E} on coarse scales. (ii) We have to take into account that the set of distances E_{ij} is discrete

such that \mathcal{N}_i does not increase smoothly but in discrete steps. In fact, it is essential to take into account that the distance to the nearest neighbor is always finite. In an analog physical model, this would correspond to a finite ‘energy gap’ between the ground and first excited state. (iii) Finally, it must be taken into account that the number of states is finite. These requirements can be met by a staircase function with steps of regular position and size. For the time being, we restrict ourselves to networks where the number of nodes can be written as $N = (M + 1)(M + 2)/2$ with $M \in \mathbb{N}$. The function $\mathcal{N}_i(\hat{E})$ can then be approximated by

$$\mathcal{N}_{\text{st}}(\hat{E}) = \sum_{m=0}^M (m + 1) \Theta(\hat{E} - mE_0), \quad (37)$$

where $E_0 = 1/\sqrt{4N}$ is the expected value of the distance to the nearest neighbor on a two-dimensional plane with node density $\rho = N$. Using this approximation, the partition function can be computed as

$$\begin{aligned} Q_{\text{st}} &= \sum_{m=0}^M (m + 1) e^{-\beta E_0 m} \\ &= \frac{1 - (M + 2)e^{-\beta E_0(M+1)} + (M + 1)e^{-\beta E_0(M+2)}}{(1 - e^{-\beta E_0})^2}. \end{aligned} \quad (38)$$

We test this approximation in figure 5 for a sample network with $N = 105$ nodes and find a very good agreement with the numerically exact values.

For large networks and low effective temperatures, we can further simplify expression (38) by noting that $e^{-\beta E_0(M+1)}/e^{-\beta E_0} \rightarrow 0$ for $\beta \rightarrow \infty$ or in large networks $M \rightarrow \infty$. We then obtain

$$Q_{\text{st}} \sim \frac{1}{(1 - e^{-\beta E_0})^2}. \quad (39)$$

In this limit, the entropy can be computed from equation (34) as

$$H_{\text{st}} \sim -2 \ln(1 - e^{-\beta E_0}) + \frac{2\beta E_0 e^{-\beta E_0}}{1 - e^{-\beta E_0}}. \quad (40)$$

We find that the entropy vanishes for low effective temperatures,

$$H_{\text{st}} \rightarrow 0 \quad \text{for} \quad \beta \rightarrow \infty,$$

indicating that all nodes i choose a single supplier. In fact, the production is local in this limit.

The entropy differs substantially from zero when βE_0 is of the order of unity leading to the estimate $\beta_{\text{crit}} \approx E_0^{-1}$ for the critical value. A slightly more accurate approximation can be obtained by computing the value for which the entropy H equals half of its maximum value which yields the implicit condition

$$H_{\text{st}}(\beta_{\text{crit}}) = \frac{1}{2} \ln(N). \quad (41)$$

For higher values of the effective temperature (lower values of β), the approximation (40) is no longer valid as indicated in figure 5

D. From centralized to diverse production

We finally consider the transition between the diverse (III) and the centralized production regime (II). This transition is driven by the competition of the two contributions to the utility function (2) – the preference for low costs and the preference for a diverse supply. Diverse production is favored if the second term is sufficiently strong, i.e. if the weight parameter (the effective temperature) \mathcal{T} exceeds a critical value $\mathcal{T}_{\text{crit}}$, cf. figure 3. This critical value can be estimated by comparing the utility function in the two regimes.

If production is fully diversified, then the supply matrix is given by $S_{ji} = D/N$ (cf. equation. (24)). The costs and utility of a node i thus read

$$\begin{aligned} K_{i,\text{div}} &= (b_i - aD)D + p^T \bar{E}_i D \\ \mathcal{U}_{i,\text{div}} &= \mathcal{T} \ln(N) - K_{i,\text{div}}, \end{aligned}$$

where \bar{E}_i is the average distance from node i to all other nodes, $\bar{E}_i = N^{-1} \sum_j E_{ij}$. If production is fully centralized at a node n , then the supply matrix is given by $S_{ji} = D\delta_{jn}$ using the Kronecker delta symbol (cf. equation (22)). In this case, the costs and utility of a node i read

$$\begin{aligned} K_{i,\text{cen}} &= (b_n - aND)D + p^T E_{in} D \\ \mathcal{U}_{i,\text{cen}} &= -K_{i,\text{cen}}. \end{aligned}$$

We expect the production to be purely centralized when $\mathcal{U}_{i,\text{cen}} > \mathcal{U}_{i,\text{div}}$ for all nodes i and to be diverse if $\mathcal{U}_{i,\text{div}} > \mathcal{U}_{i,\text{cen}}$ for all i . If scale effects are sufficiently strong, then the differences

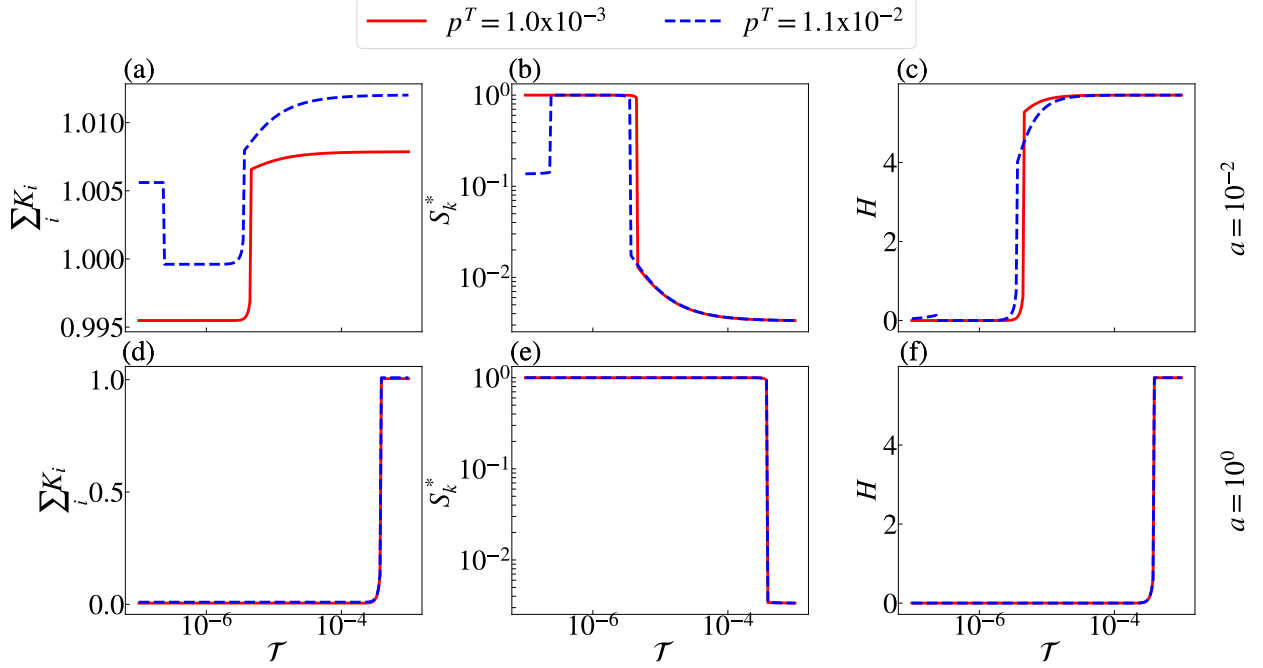


Figure 6. Transition from diverse to centralized production. Results are shown for a single instance of the transportation network, comparing the case of (a-c) weak scale effects and (d-f) strong scale effects as well as different values of the specific transportation costs p^T (red solid vs. blue dashed line). We show (a,d) the total costs $\sum_i K_i$, (b,e) the production of the busiest node $S_k^* = \max_k S_k$ and (c,f) the entropy H_i averaged over all nodes. The transition is very sharp and occurs at a critical value of the effective temperature given by equation (42). A non-monotonous behavior of S_k^* is found for $a = 10^0$ and $p^T = 1.1 \times 10^{-2}$, which is discussed in the text.

between the nodes i are negligible and the transition is abrupt. We expect the transition to take place at a critical temperature $\mathcal{T}_{\text{crit}}$ given by

$$\begin{aligned} \mathcal{U}_{i,\text{central}}(\mathcal{T}_{\text{crit}}) &\approx \mathcal{U}_{i,\text{diverse}}(\mathcal{T}_{\text{crit}}), \\ \Rightarrow \mathcal{T}_{\text{crit}} &\approx \frac{K_{i,\text{div}} - K_{i,\text{cen}}}{\ln(N)}. \end{aligned}$$

Neglecting the inhomogeneities in the b_i and the transportation distances, we finally obtain

$$\mathcal{T}_{\text{crit}} \approx \frac{a(N-1)D^2}{\ln(N)}. \quad (42)$$

We conclude that the transition between diverse and centralized production is driven by the competition of scale effects scaling linearly in a and the preference for diversity scaling linearly in \mathcal{T} , while transportation effects play a negligible role. Hence, the critical effective temperature $\mathcal{T}_{\text{crit}}$ scales linearly in a , while it is largely independent of the specific

transportation costs p^T . However, this reasoning is only valid as long as local production is not competitive, i.e. as long as p^T is small enough.

A surprising behavior is found for weak scale effects and intermediate value of the specific transportation costs p^T (Figure 6, upper row, dashed line). We find that the maximum production S^* jumps to one when the effective temperature \mathcal{T} increases above approximately 10^{-6} . That is, an increase in the preference for product diversification leads to a decrease in product diversification. This counter-intuitive behavior is a consequence of the multistability of the economic system. Two Nash equilibria exist for $\mathcal{T} \ll 10^{-6}$, one with an incomplete and one with a complete centralization of production. Due to the design of our numerical experiments the initial state features an incomplete centralization. An increase in \mathcal{T} fosters trade, strengthening one producer at the expense of another one. Eventually, the Nash equilibrium with incomplete centralization becomes unstable, and the system relaxes to the centralized equilibrium, offering lower total costs due to scale effects. Notably, a further increase of the effective temperature finally leads to a fully diversified production as expected.

E. Comparison to numeric results

As a final step of our analysis, we compare the analytical estimates for the location of the phase boundaries to the numerical results in Figure 7. We find that the estimate (41) for the phase boundary between the localized and diversified phase accurately matches the numerical results with no visible differences. The estimate (42) slightly overestimates the critical value $\mathcal{T}_{\text{crit}}$ for the transition from centralized to diversified. However, the analytical estimate faithfully reproduces the order of magnitude of $\mathcal{T}_{\text{crit}}$ as well as the scaling with the parameter a . Similarly, the estimate (30) provides a fair overall estimate for the critical value p_{crit}^T for the transition from localized to centralized production. The scaling with a is overestimated such that analytical estimates are larger than the numerically exact values for large a . This is not surprising as we expect a smooth crossover between the two different scaling regimes. For medium to large values of a , we expect a proportional scaling of p_{crit}^T with a as described by (30). In contrast, p_{crit}^T should tend to a constant for small values of a as there is still a (continuous) centralization at a finite p_{crit}^T due to the small inhomogeneity in the b_i .

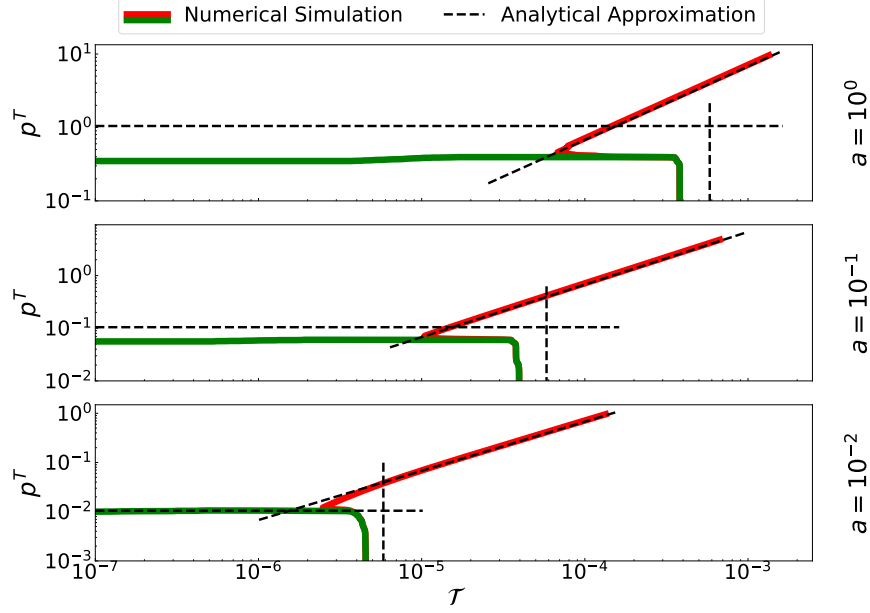


Figure 7. Comparison of numerical results and analytic estimates for the location of phase transitions in terms of the parameters p^T and τ . Green and red lines show the numerical results as established in Figure 3. Black dashed lines show the corresponding analytical estimates according to equation 30, 41, and 42. The strength of the scale effects is varied as $a = 10^0$ (top panel), $a = 10^{-1}$ (middle panel) and $a = 10^{-2}$ (bottom panel).

V. CONCLUSION AND OUTLOOK

In this article, we have established a model for the formation of trade networks based on the decisions of economic agents. The model combines two driving factors for the emergence of trade: On the supply side, trade is established if regional differences in production costs exceed the transportation costs. On the demand side, the preference for differentiated goods fosters trading even if this increases costs.

The developed model shows strong connections to ensembles in statistical thermodynamics, with the utility function resembling the Helmholtz free energy up to a sign. However, there is one important difference: The economic agents optimize their utility functions *individually*, where the respective utility functions are interdependent due to the economic scale effects. Hence, the common equilibrium of statistical physics must be generalized to a Nash equilibrium. Nevertheless, statistical thermodynamics provides essential concepts to compute the equilibrium states and to understand the emergence of a trade network.

We have shown that the model bears three different regimes of trade. If transportation costs are high and the preference for product differentiation is weak, then all goods are produced locally. A trade network can emerge in two different ways rooted in either the supply or demand side. Decreasing transportation costs make it cheaper to import goods, thus leading to a centralization of production and a directed star-like trade network. An increasing preference for product differentiation drives the emergence of bilateral trade and eventually leads to an all-to-all coupled trade network. We have developed a comprehensive analytical theory of the transitions between these regimes and derived analytical estimates for critical parameter values. Remarkably, the transition to a phase with centralized production can be continuous as well as discontinuous if economic scale effects are strong enough.

The model describes some essential mechanisms in the formation of trade networks – but of course it cannot capture all facets of this complex process. For instance, production will either be centralized completely or not at all when transportation costs continue to decrease. In reality, one often observes multi-center structures, for example in urban systems [24, 25] as a result of spatial constraints or congestion at high levels of centralization. In the proposed modeling framework, this would be possible if scale effects saturated or if transportation capacities were limited. From a more fundamental viewpoint, the model assumes a fixed demand at any node in contrast to other economic models. For instance, the celebrated Dixit-Stiglitz model assumes a fixed budget instead [26]. From a statistical viewpoint, a thorough treatment of the thermodynamic limit remains challenging due to the different scaling behaviors in the utility function. This analysis is well beyond the scope of the present analysis, so we have focused on finite systems.

Appendix A: Proof of discontinuous transition

In this appendix we proof the existence of a discontinuous transition in a single step from Sec. IV A.

We first consider the purchases of node $i = 2$, that may choose to purchase from node $j = 1$ or produce locally. By an explicit computation, we can show that local production ($S_{22} = D$, $S_{12} = 0$) is cheaper for $p^T > p_{\text{crit}}^T$. Importing goods ($S_{22} = 0$, $S_{12} = D$) is cheaper for $p^T < p_{\text{crit}}^T$.

Due to the ordering of the nodes we can conclude two further statements: (i) Node $i = 2$

will change its purchases to buy at node $j = 1$, while purchasing at another node $\ell \geq 3$ provides no benefits. (ii) Node $i = 2$ is the first one to change its purchases. That is, production is fully locally ($S_{\ell,\ell} = D$ for all nodes $\ell = 1, \dots, N$) for $p^T > p_{\text{crit}}^T$.

Now consider the consequences of node $i = 2$ changing its purchases at $p^T = p_{\text{crit}}^T$. Node $i' = 3$ can either buy locally at an effective price

$$p_{33}^{\text{eff}} = b_3 - aD \quad (\text{A1})$$

or at node $j = 1$ at an effective price

$$p_{13}^{\text{eff}} = b_1 - 3aD + p_{\text{crit}}^T E_{13}. \quad (\text{A2})$$

By our assumption (29), we find that $p_{13}^{\text{eff}} < p_{33}^{\text{eff}}$ such that node $i' = 3$ changes its purchases from local to import simultaneously with node $i = 2$. The same argument now applies to all nodes $i'' = 4 \dots, N$. Hence, we conclude that at $p^T = p_{\text{crit}}^T$ all nodes simultaneously change their purchases such that we find

$$\text{for } p^T > p_{\text{crit}}^T : \quad S_{ii} = D, \quad (\text{A3})$$

$$\text{for } p^T < p_{\text{crit}}^T : \quad S_{1i} = D, \quad (\text{A4})$$

for all nodes $i = 1 \dots, N$.

Appendix B: Entropy and partition function

In this appendix we briefly recall the relation of the entropy and the partition function (35). In particular, we show that the expression (34) for the entropy H_i is equivalent to the definition (3). Differentiating the partition function Q_i with respect to β yields

$$\begin{aligned} -\frac{\partial}{\partial \beta} \ln(Q_i) &= -\frac{1}{\sum_{l=1}^N e^{-\beta E_{li}}} \frac{\partial}{\partial \beta} \sum_{j=1}^N e^{-\beta E_{ji}}, \\ &= \sum_{j=1}^N \frac{e^{-\beta E_{ji}}}{\sum_{l=1}^N e^{-\beta E_{li}}} E_{ji}, \\ &= \sum_{j=1}^N \frac{S_{ji}}{D} E_{ji}. \end{aligned} \quad (\text{B1})$$

Similarly, we can show that

$$\begin{aligned}
-\frac{\partial}{\partial \beta^{-1}}(-\beta^{-1} \ln Q_i) &= \ln Q_i - \beta \frac{\partial}{\partial \beta} \ln Q_i \\
&= \ln Q_i + \beta \sum_{j=1}^N \frac{S_{ji}}{D} E_{ji}.
\end{aligned} \tag{B2}$$

Next, we start from the definition of entropy,

$$\begin{aligned}
H_i &= - \sum_{j=1}^N \frac{S_{ji}}{D} \ln \frac{S_{ji}}{D} \\
&= - \sum_{j=1}^N \frac{e^{-\beta E_{ji}}}{\sum_{l=1}^N e^{-\beta E_{li}}} \ln \frac{e^{-\beta E_{ji}}}{\sum_{l=1}^N e^{-\beta E_{li}}} \\
&= - \sum_{j=1}^N \frac{e^{-\beta E_{ji}}}{\sum_{l=1}^N e^{-\beta E_{li}}} \left[\ln e^{-\beta E_{ji}} - \ln \sum_{l=1}^N e^{-\beta E_{li}} \right] \\
&= \sum_{j=1}^N \frac{e^{-\beta E_{ji}}}{\sum_{l=1}^N e^{-\beta E_{li}}} \beta E_{ji} + \ln \left(\sum_{l=1}^N e^{-\beta E_{li}} \right) \sum_{j=1}^N \frac{e^{-\beta E_{ji}}}{\sum_{l=1}^N e^{-\beta E_{li}}} \\
&= \beta \sum_{j=1}^N \frac{S_{ji}}{D} E_{ji} + \ln(Q_i),
\end{aligned} \tag{B3}$$

which coincides with the expression (B2).

ACKNOWLEDGEMENTS

We thank Joahannes Többen for stimulating discussions. We gratefully acknowledge support from the German Federal Ministry of Education and Research (BMBF) via the grant *CoNDyNet* with grant no. 03EK3055, the Helmholtz Association via the grant *Uncertainty Quantification – From Data to Reliable Knowledge (UQ)* with grant no. ZT-I-0029, and the Deutsche Forschungsgemeinschaft (DFG, German Research Foundation) with grant No. 491111487.

-
- [1] P. Krugman, *Geography and trade* (MIT press, 1992).
 - [2] F. Schweitzer, G. Fagiolo, D. Sornette, F. Vega-Redondo, A. Vespignani, and D. R. White, Economic networks: The new challenges, *Science* **325**, 422 (2009).

- [3] P. Gai, A. Haldane, and S. Kapadia, Complexity, concentration and contagion, *Journal of Monetary Economics* **58**, 453 (2011).
- [4] D. Helbing, Globally networked risks and how to respond, *Nature* **497**, 51 (2013).
- [5] D. Guan, D. Wang, S. Hallegatte, S. J. Davis, J. Huo, S. Li, Y. Bai, T. Lei, Q. Xue, D. Coffman, *et al.*, Global supply-chain effects of covid-19 control measures, *Nature Human Behaviour* **4**, 577 (2020).
- [6] M. E. Newman, The structure and function of complex networks, *SIAM review* **45**, 167 (2003).
- [7] R. Pastor-Satorras, M. Rubi, and A. Diaz-Guilera, *Statistical mechanics of complex networks*, Vol. 625 (Springer Science & Business Media, 2003).
- [8] S. Havlin, D. Y. Kenett, E. Ben-Jacob, A. Bunde, R. Cohen, H. Hermann, J. Kantelhardt, J. Kertész, S. Kirkpatrick, J. Kurths, *et al.*, Challenges in network science: Applications to infrastructures, climate, social systems and economics, *The European Physical Journal Special Topics* **214**, 273 (2012).
- [9] D. J. Watts and S. H. Strogatz, Collective dynamics of ‘small-world’ networks, *Nature* **393**, 440 (1998).
- [10] A.-L. Barabási and R. Albert, Emergence of scaling in random networks, *science* **286**, 509 (1999).
- [11] M. E. J. Newman, *Networks: An introduction* (Oxford University Press, Oxford, 2010).
- [12] E. Katifori, G. J. Szöllősi, and M. O. Magnasco, Damage and fluctuations induce loops in optimal transport networks, *Physical review letters* **104**, 048704 (2010).
- [13] F. Kaiser, H. Ronellenfitsch, and D. Witthaut, Discontinuous transition to loop formation in optimal supply networks, *Nature Communications* **11**, 1 (2020).
- [14] P. R. Krugman and M. Obstfeld, *International economics: Theory and policy* (Pearson Education, 2009).
- [15] P. R. Krugman, Increasing returns, monopolistic competition, and international trade, *Journal of international Economics* **9**, 469 (1979).
- [16] S. P. Anderson, A. De Palma, and J.-F. Thisse, *Discrete choice theory of product differentiation* (MIT press, 1992).
- [17] K. Lancaster, The economics of product variety: A survey, *Marketing science* **9**, 189 (1990).
- [18] S. P. Anderson and A. De Palma, The logit as a model of product differentiation, *Oxford Economic Papers* **44**, 51 (1992).

- [19] F. Matějka and A. McKay, Rational inattention to discrete choices: A new foundation for the multinomial logit model, *American Economic Review* **105**, 272 (2015).
- [20] M. Schröder, J. Nagler, M. Timme, and D. Witthaut, Hysteretic percolation from locally optimal individual decisions, *Physical review letters* **120**, 248302 (2018).
- [21] C. Han, D. Witthaut, M. Timme, and M. Schröder, The winner takes it all—competitiveness of single nodes in globalized supply networks, *PloS one* **14**, e0225346 (2019).
- [22] D. Achlioptas, R. M. D’Souza, and J. Spencer, Explosive percolation in random networks, *science* **323**, 1453 (2009).
- [23] R. M. D’Souza and J. Nagler, Anomalous critical and supercritical phenomena in explosive percolation, *Nature Physics* **11**, 531 (2015).
- [24] M. Fujita and H. Ogawa, Multiple equilibria and structural transition of non-monocentric urban configurations, *Regional science and urban economics* **12**, 161 (1982).
- [25] R. Louf and M. Barthélemy, Modeling the polycentric transition of cities, *Physical Review Letters* **111**, 198702 (2013).
- [26] A. K. Dixit and J. E. Stiglitz, Monopolistic competition and optimum product diversity, *The American economic review* **67**, 297 (1977).